Compositional Characterization and Color Genesis of Precious Coral Based on Multi-Spectroscopic Techniques

Yushu Yang , Ying Guo * , Zhe Hu , Jiayang Han

Posted Date: 23 April 2026

doi: 10.20944/preprints202604.1664.v1

Keywords: precious coral; polyene pigment; FTIR spectroscopy; raman spectroscopy; UV-Vis spectroscopy

 doi:10.20944/preprints202604.1664.v1

Article

Compositional Characterization and Color Genesis of Precious Coral Based on Multi-Spectroscopic Techniques

Yushu Yang [1], Ying Guo *, Zhe Hu and Jiayang Han

School of Gemology, China University of Geosciences, Beijing 100083, China

* Correspondence: 2001011459@cugb.edu.cn

Abstract

The color origin of precious coral, a highly valued organic polycrystalline gemstone, has long remained elusive. In this study, an integrated approach employing spectrophotometry, Raman, FTIR, and UV-Vis spectroscopy, coupled with Spearman correlation analysis, was utilized to investigate a color-graded series of precious coral samples ranging from white to red. The results demonstrate that the calcareous skeleton consists exclusively of calcite. The actual chromophores are identified as a blend of multiple distinct polyene species, characterized by Raman shifts at 1126 and 1515 cm^{-1}. Inherently exhibiting a red-orange hue, the progressive accumulation of these polyenes drives a systematic color transition from orange to red.Both absorption bands at 314 nm and 532 nm in the UV-Vis spectra originate from the polyene pigment molecules. Specifically, the broad 532 nm band is dominated by π-π^* electronic transitions. As the pigment concentration increases, this band exhibits pronounced broadening and enhancement, accompanied by a redshift of the maximum absorption peak. This spectral evolution leads to an intensified absorption in the yellow-orange region, elucidating the intrinsic mechanism underlying the color transition of precious coral from orange to red with increasing pigment content. This work lays a solid foundation for the non-destructive identification of precious corals and future research on their color genesis.

Keywords: precious coral; polyene pigment; FTIR spectroscopy; raman spectroscopy; UV-Vis spectroscopy

1. Introduction

Precious coral, a highly valued organic gemstone[1], exhibits a continuous spectrum of hues—spanning a gradual transition from white, pink, and orange to red—rather than being confined solely to red. Its utilization by humans dates back over 7,000 years[2]. Across diverse civilizations, including ancient Greek, Roman, Christian, Buddhist, and Islamic cultures, precious coral has held profound significance, historically endowed with auspicious connotations such as protection, sanctity, wisdom, and prosperity[3].

Precious coral is the colonial skeleton of certain species within the Coralliidae family, primarily composed of an inorganic phase (calcium carbonate) and an organic matrix comprising carbohydrates, lipids, proteins, and pigments such as carotenoids and polyenes[4]. In terms of biomineralization, corals can be classified into calcite and aragonite types based on their calcareous skeletal composition. Early academic consensus generally held that white corals belonged to the aragonite type, whereas red corals belonged to the calcite type. However, subsequent in-depth studies have demonstrated the limitations of this view, revealing that many red corals are actually aragonitic, while numerous white corals are calcitic[5,6].

The origin of the vibrant red color in precious coral has long been a focal point in academic research, with investigative approaches primarily falling into two categories: ex-situ pigment extraction and in-situ spectral analysis. Regarding pigment extraction, Fox et al. (1972) attempted

 doi:10.20944/preprints202604.1664.v1

extractions from various corals; however, due to the tight binding between the pigments and the organic matrix, none of the organic solvents tested achieved effective separation[7]. Cvejic et al. (2007) reported the successful extraction of precious coral pigments, identifying them as canthaxanthin[8], though this conclusion failed to gain widespread acceptance in the scientific community[9]. Despite the controversy surrounding their assertion that canthaxanthin is the principal pigment, this study did confirm the actual presence of canthaxanthin within precious coral. Subsequently, Bracco et al. (2016) made further extraction attempts, but the low extraction efficiency yielded pigment quantities insufficient for subsequent molecular structural characterization and identification[10].

Compared to the challenges inherent in ex-situ extraction, in-situ spectral techniques—particularly Raman spectroscopy—have achieved substantial progress in elucidating the coloration mechanisms of precious coral. As early as the 1980s, Merlin's team investigated the Raman spectra of various carotenoids[11], and subsequent research extended to the actual coloring pigments in precious corals, ultimately identifying them as polyene pigments[12].

Following this, advancements unfolded in two main dimensions. In practical application, Karampelas and Smith established Raman spectroscopy as an effective, non-destructive tool for identifying precious corals[13,14]. Furthermore, Yang et al. conducted comparative analyses on commercial varieties such as Aka, Sardinia, and Momo corals; observing consistent Raman peak positions across these samples, they postulated that different species within the Coralliidae family might share the same class of coloring pigments[15]. On a theoretical level, scholars including Kupka, Bergamonti, and Brambilla introduced Density Functional Theory (DFT) to simulate the Raman spectra of precious corals, deducing that the carbon-carbon double bond (C=C) conjugated chain length of this polyene pigment is approximately 10 to 11 units[6,16–18].Additionally, the applicability of Raman spectroscopy extends beyond precious corals, playing an irreplaceable role in the study of shells[19–21] and pearls [22,23].

Compared to the extensive application of Raman spectroscopy in studying precious coral pigments, the utilization of infrared (IR) and ultraviolet-visible (UV-Vis) spectroscopies remains relatively limited in this field. In previous studies, IR spectroscopy has predominantly focused on the calcareous skeleton of precious corals [24,25], whereas UV-Vis spectroscopy has primarily been employed to quantify polyene pigments in other domains[26].

A comprehensive review of existing in-situ spectroscopic studies on precious coral, despite their fruitful outcomes, reveals several notable deficiencies. Firstly, previous research has been confined to discrete color samples, making it difficult to establish a rigorous correspondence between polyene spectral signals and pigment content, thereby precluding conclusive correlations. Furthermore, in terms of pigment-related research, color characterization has predominantly relied on visual assessments. This approach is not only susceptible to interference from ambient lighting and observer subjectivity, but also lacks quantifiability, rendering the documentation and expression of color highly ambiguous.

In light of these limitations, the present study selected a suite of precious coral samples encompassing a continuous color gradient from white to deep red. A systematic investigation was conducted using an integrated approach comprising Raman, FTIR, and UV-Vis spectroscopies. Simultaneously, colorimetric analysis was introduced to precisely quantify the macroscopic color data, and Spearman's correlation coefficients were employed to evaluate the relationships among these parameters. This study aims to establish a multidimensional correlation among color, pigment molecules, and spectral characteristics. Ultimately, it seeks to definitively confirm the intrinsic links between the Raman signals (and their corresponding pigment molecules) and the color of precious coral, and to elucidate the genesis of its broad color spectrum through a spectroscopic lens.

2. Materials and Methods

2.1. Materials

 doi:10.20944/preprints202604.1664.v1

The samples used in this study comprised 19 precious corals sourced from the Pacific Ocean. They exhibited diverse morphologies, including oval, teardrop, branching, and irregular massive forms. The surfaces were polished, displaying a bright vitreous luster, and the samples ranged from translucent to semi-transparent. Their colors spanned a complete gradient from white to deep red, and the samples were sequentially numbered from 1 to 19 in order of increasing color depth. Physical photographs of the samples are presented in Figure 1.

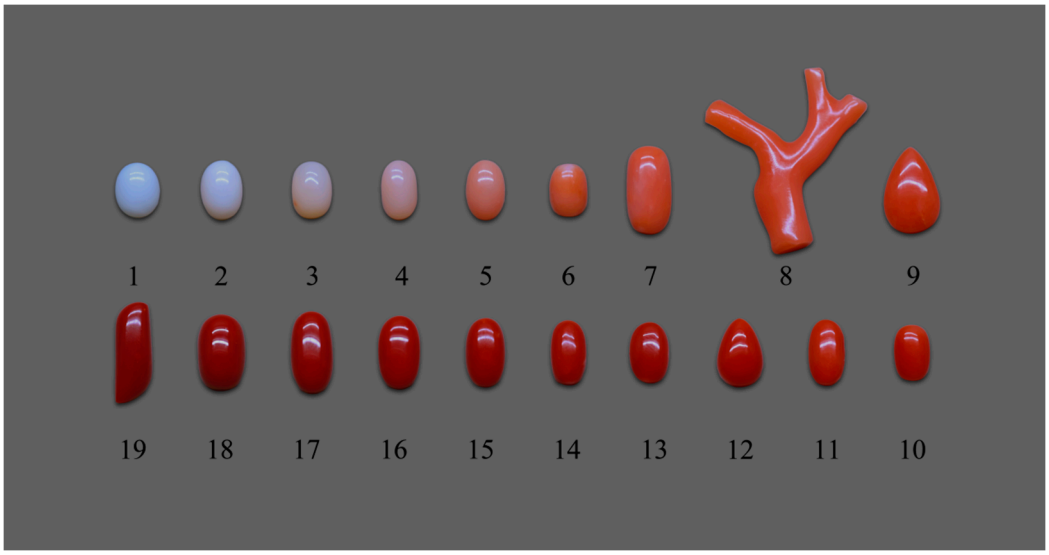

Figure 1. Photographs of the precious coral samples used in this study, numbered 1–19 in order of increasing color depth.

2.2. Experimental Methods and Instrumentation

Spectrophotometry

Color measurements were performed in Room 410 of the School of Gemmology, China University of Geosciences (Beijing), using an X-Rite SP62 integrating sphere spectrophotometer. The measurement conditions were set as follows: a D65 standard illuminant, the specular component excluded (SCE) mode, a 2° observer viewing angle, and a measurement spot diameter of 4 mm. The single measurement time was 2.5 s, with a wavelength sampling interval of 10 nm over an acquisition range of 400–700 nm. To minimize errors, each sample was measured three times and the average value was calculated. An N6 neutral gray background was used for the tests, and the color data were recorded and exported in the CIE 1976 L*a*b* uniform color space.

*CIE 1976 L*a*b* Uniform Color Space*

The CIE 1976 L*a*b* color space exhibits excellent visual uniformity[27]. This system is composed of the lightness index L* and the chromaticity coordinates a* and b*. Specifically, L* represents lightness; a* represents the red-green axis (+a* indicates red, while -a* indicates green); and b* represents the yellow-blue axis (+b* indicates yellow, while -b* indicates blue). Based on these parameters, the chroma C* and hue angle h° can be further derived from the a* and b* values using the following formulas[28]:

$$C^* = \sqrt{a^{*2} + b^{*2}} \quad (1)$$

$$h° = \arctan\frac{b^*}{a^*} \quad (2)$$

Raman Spectroscopy

Raman spectroscopy was performed at the laboratory of the School of Gemmology, China University of Geosciences (Beijing). The measurements were conducted using a LabRAM HR Evolution micro-Raman spectrometer. The experimental parameters were set as follows: a 532 nm

 doi:10.20944/preprints202604.1664.v1

Ar^+ ion laser was utilized as the excitation source, the spectral acquisition range was 100–4000 cm^{-1}, and the laser spot diameter was 1298 nm.

Fourier Transform Infrared (FTIR) Spectroscopy

FTIR measurements were performed at the laboratory of the School of Gemmology, China University of Geosciences (Beijing), using a Bruker Tensor 27 spectrometer. Data were collected in reflectance mode with a spectral resolution of 4 cm^{-1} over the range of 400–4000 cm^{-1}. For a single acquisition, the scanning time was 32 s, the aperture was set to 6 mm, and the scanning speed was 10 Hz.

Ultraviolet-Visible (UV-Vis) Spectroscopy

UV-Vis measurements were conducted at the laboratory of the School of Gemmology, China University of Geosciences (Beijing), using a UV-3600 spectrophotometer. Data were collected in reflectance mode over a spectral scanning range of 200–900 nm. The instrumental parameters were set as follows: a slit width of 20 nm, an integration time of 0.5 s, and the high-speed scanning mode was employed.

3. Results

3.1. Color Analysis

The fundamental color-forming mechanism of an object is essentially the interaction between light and matter: upon illumination, the object selectively absorbs specific wavelengths of light, while the remaining wavelengths are reflected and stimulate the human visual system, thereby generating the perception of color.

Under the D65 standard illuminant, the color parameters of the 19 precious coral samples are distributed as follows: the red-green chromaticity index a* ranges from -2.15 to 37.17, and the yellow-blue chromaticity index b* ranges from 4.31 to 25.80. Their projections on the a*b* plane are illustrated in Figure 2A. The lightness index L* varies from 31.95 to 88.64, falling within the medium-to-high lightness range. The chroma C* spans from 4.82 to 43.93, with higher values indicating greater color saturation. Additionally, the hue angle h° ranges from 24.49° to 116.51°.

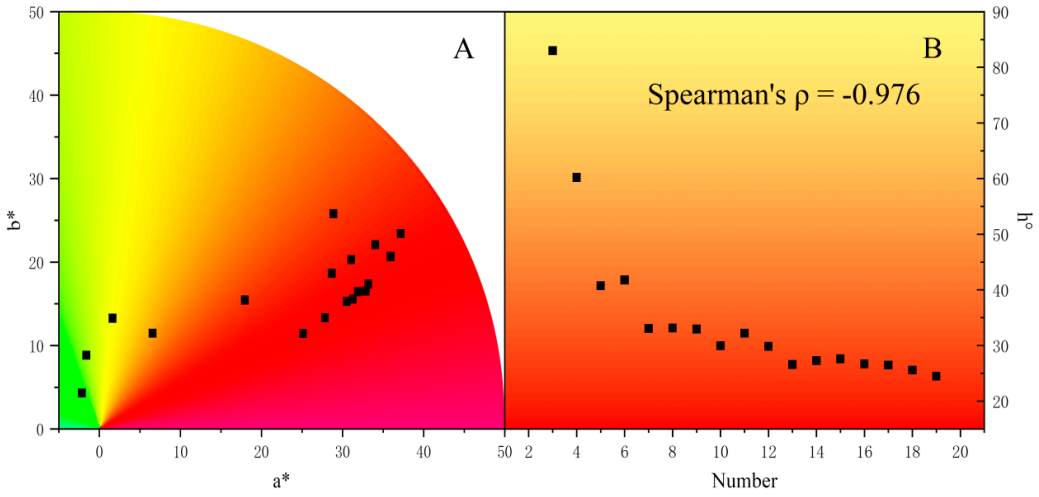

Figure 2. (A) Projections of a* and b* for samples 1–19; (B) Variation of hue angle (h°) with the pigment content in samples 3–19.

As shown in Figure 2A, the chromaticity coordinates of the vast majority of precious coral samples fall within the first quadrant of the a*b* plane (i.e., the red-yellow color region). Only samples No. 1 and No. 2 deviate from this region, distributing in the yellow-green color region. These two samples appear white, and their a* values are negative due to an extremely low content of organic pigments. The a* values of all other samples are positive.

 doi:10.20944/preprints202604.1664.v1

The experimental samples were sequentially numbered based on their visually observed color depth. Given that this visual depth is positively correlated with the internal pigment content, the sample sequence number was utilized as a proxy indicator for both color depth and pigment concentration. Figure 2B illustrates the mapping relationship between the sequence numbers of the samples (Nos. 3–19) and their hue angles (h°). The results reveal a significant negative correlation between the two (Spearman's ϱ = -0.976). This extremely strong correlation intuitively demonstrates that as the pigment content increases, the hue angle (h°) decreases, causing the hue to shift from yellow-orange to true red.

3.2. Raman Spectroscopy

Based on the inelastic scattering (Raman scattering) of monochromatic light by matter, Raman spectroscopy sensitively captures molecular vibrational and rotational information. It serves as a powerful tool for elucidating chemical compositions and molecular structures, and has been widely validated as an effective approach for authenticating precious corals and probing their internal organic components[13] . To further elucidate the material composition of the samples, Raman spectral analyses were conducted on all 19 precious coral specimens.

The Raman spectra of the two white samples (No. 1 and No. 2), the two aragonites, and a calcite sample are compared in Figure 3.

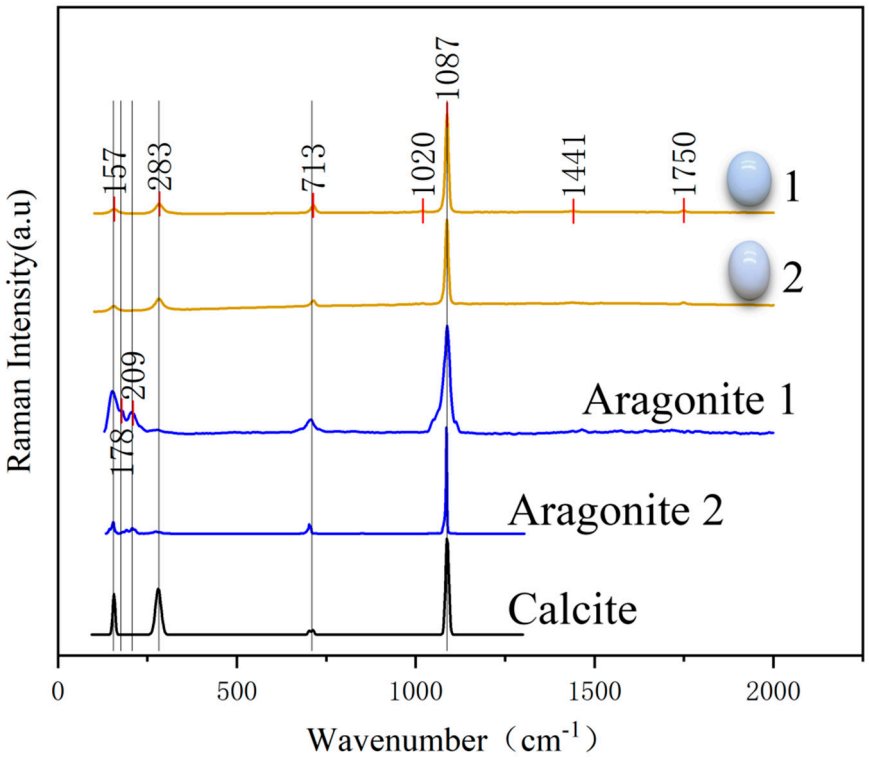

Figure 3. Raman spectra of white precious coral, aragonite, and calcite. The brownish-yellow, blue, and black lines correspond to white precious coral, aragonite, and calcite, respectively.

As shown in Figure 3, the Raman spectra of the two white samples (No. 1 and No. 2) exhibit exclusively the characteristic signals of their calcareous skeletons. Comparison with the Raman spectra of inorganic minerals reveals the absence of aragonite characteristic peaks at 178 and 209 cm^{-1} in their spectra. Conversely, the Raman shifts at 157, 283, 715, and 1087 cm^{-1} perfectly match the characteristic peaks of calcite.

The Raman spectral peaks of samples No. 1 and No. 2 are assigned as follows: the weak peaks located at 157 and 283 cm^{-1} are attributed to the translational and rotational vibrations of the calcite lattice, respectively; the signal at 1020 cm^{-1} indicates the presence of bicarbonate ions (HCO_3^-).

 doi:10.20944/preprints202604.1664.v1

Furthermore, a series of peaks at 713, 1087, 1441, and 1750 cm^{-1} all originate from the internal vibrations of carbonate ions (CO_3^{2-}), corresponding sequentially to the in-plane bending vibration, symmetric stretching vibration, asymmetric stretching vibration, and the second-overtone of the out-of-plane bending vibration[18].

Theoretically, Raman signal intensity is positively correlated with analyte concentration; however, due to interference from complex external factors—such as laser power, integration time, sample surface polish, and laser incidence angle—the absolute intensity of spectra is unsuitable for the accurate quantification of substance concentrations. Nevertheless, calcite accounts for up to 98%[29] of the mineral composition of precious coral (approximating a pure phase), meaning its concentration can be treated as a constant. Leveraging this characteristic, the present study utilized the characteristic Raman signal of calcite as an internal standard. By calculating the ratio of the characteristic peak intensity of the target analytes to the reference peak intensity of calcite (i.e., the relative intensity), the errors arising from fluctuations in testing conditions were effectively eliminated, thereby enabling the semi-quantitative analysis of the internal components of precious coral.

Using the strongest characteristic peak of calcite at 1087 cm^{-1} as an internal standard, the Raman spectra of samples No. 1–19 were normalized, and the results are presented in Figure 4. Following this treatment, the absolute intensities of all other characteristic peaks were converted into relative intensities referenced to calcite.

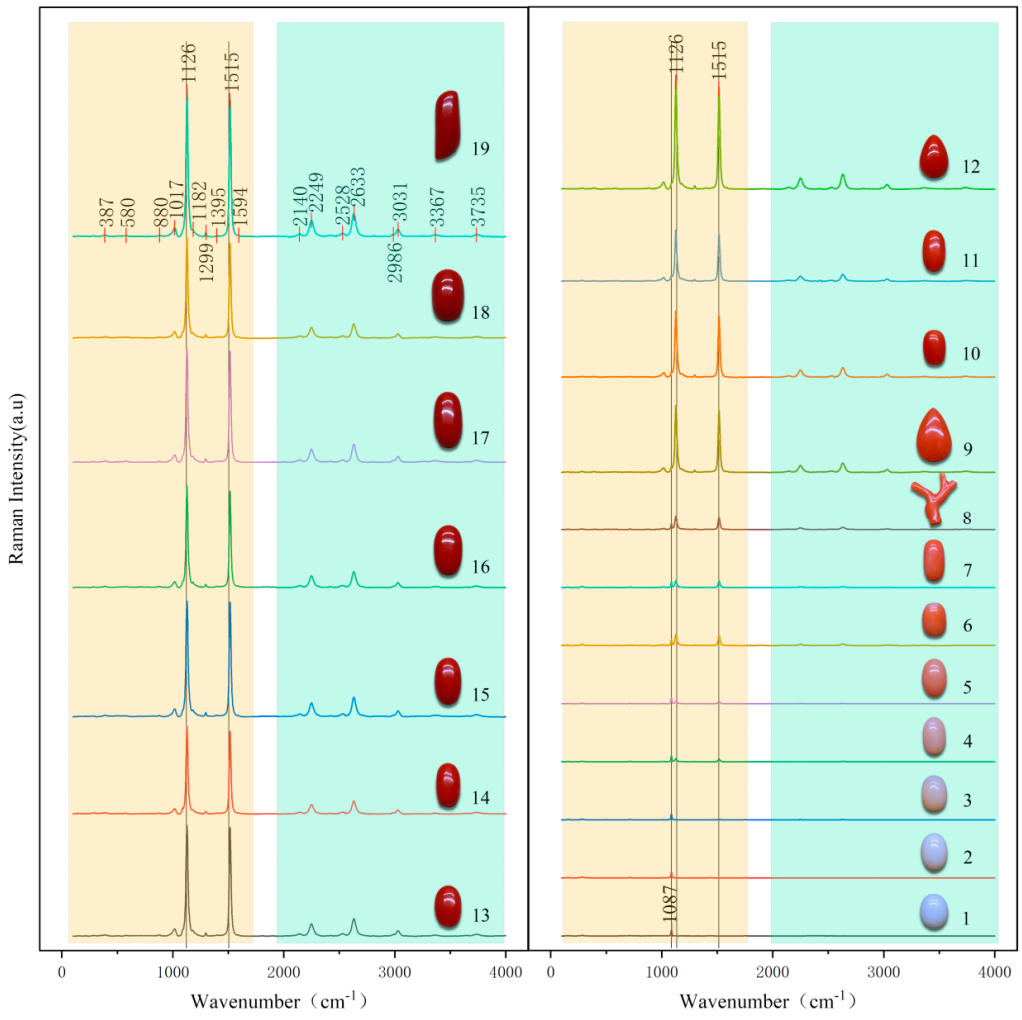

Figure 4. Normalized Raman spectra of the precious coral samples (Nos. 1–19).

 doi:10.20944/preprints202604.1664.v1

The Raman characteristic peak positions of the polyene pigments are shown in Figure 4, and the assignments are as follows:

The fundamental vibration peaks (the yellow region in Figure 4, 387–1584 cm^{-1}) are specifically assigned as follows: the peak at 1017 cm^{-1} (ν_3) originates from the rocking vibration of (–CH_3) and is degenerate with the 1120 cm^{-1} peak of calcite; the peaks at 1126 cm^{-1} (ν_2) and 1515 cm^{-1} (ν_1) correspond to the stretching vibrations of (C–C) and (C=C), respectively[12]; and the peak at 1299 cm^{-1} (ν_4) is attributed to the in-plane rocking vibration of the H atoms in (C–H)[16]. Additionally, polyene pigment signals were also observed at 387, 580, 880, 1182, 1395, 1594, and 2986 cm^{-1}, although their exact vibrational modes remain to be further confirmed.

In the high-wavenumber region (the blue region in Figure 4, 2140–3735 cm^{-1}), with the exception of 2986 cm^{-1}, all other peaks are combination bands of the fundamental peaks. These specifically include the combination bands at 2140 cm^{-1} ($\nu_2+\nu_3$), 2249 cm^{-1} ($2\nu_2$), 2528 cm^{-1} ($\nu_1+\nu_3$), 2633 cm^{-1} ($\nu_1+\nu_2$), 3031 cm^{-1} ($2\nu_1$ or $3\nu_3$ and their degenerate peaks), 3367 cm^{-1} ($\nu_1+\nu_2+\nu_3$), and 3735 cm^{-1} ($\nu_1+2\nu_2$)[12].

The normalized spectra (Figure 4) clearly illustrate the dynamic evolution of the polyene Raman signals with increasing color depth. In the virtually pigment-free white samples (No. 1 and No. 2), only the characteristic calcite peak at 1087 cm^{-1} is present. Weak polyene signals begin to emerge in the light pink samples (No. 3–5), with intensities lower than that of the 1087 cm^{-1} calcite peak. As the sample color transitions to orange-red (No. 6–8) and further to red-to-dark-red (No. 9–19), the polyene Raman signals exhibit a remarkable increase. Not only do they vastly exceed the intensity of the 1087 cm^{-1} calcite peak, but in samples No. 9–19, they also alter the spectral profile: the intense principal peak at 1126 cm^{-1} envelops the 1087 cm^{-1} peak, reducing it to a shoulder peak.

Relying solely on visual inspection to estimate spectral signal intensity is inherently imprecise; moreover, the visual perception of color is susceptible to external environmental factors, such as the spectral power distribution of the light source, illumination intensity, and the brightness and color of the observation background. To eliminate the bias associated with subjective visual assessments of spectral intensity and color variation, and to derive more objective conclusions, this study utilized the integrated intensity of the characteristic polyene peak at 1515 cm^{-1} as the indicator of polyene concentration. Concurrently, the visual ranking of color depth and the instrumentally measured lightness index (L*) were jointly employed as indicators of pigment concentration in the precious coral. Correlation analyses were then performed between the integrated intensity of the 1515 cm^{-1} peak and the visual ranking as well as the L* values, with the results presented in Figure 5.

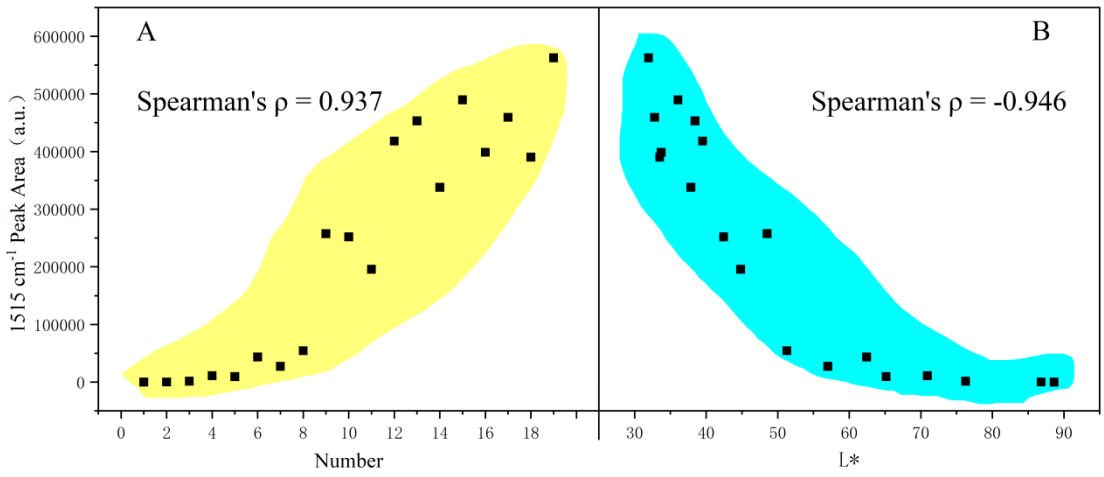

Figure 5. Projections of the 1515 cm^{-1} peak intensity against (A) the visual ranking and (B) the L* value.

The statistical analysis (Figures 5A and 5B) reveals a highly significant positive correlation between the integrated intensity of the characteristic polyene peak at 1515 cm^{-1} and the visual ranking (Spearman's $\varrho = 0.937$), as well as a highly significant negative correlation with the lightness value L* (Spearman's $\varrho = -0.946$). These two highly significant correlations—one positive and one negative—

 doi:10.20944/preprints202604.1664.v1

validate the feasibility of using the lightness value (L*) measured by a spectrophotometer as a substitute for the visually perceived color depth to inversely indicate pigment content.

3.3. Infrared Spectroscopy

IR spectroscopy achieves material analysis based on the selective absorption of infrared light by molecules during vibrational energy level transitions. Many vibrational modes that are restricted or exhibit weak signals in Raman spectroscopy often show strong responses in IR spectroscopy, making the two techniques highly complementary in research. In this study, reflection-based IR spectra of coral samples No. 1–19 were collected over the range of 400–4000 cm^{-1}. To effectively eliminate the interference of physical factors—such as sample surface roughness and test coverage area—on the absolute spectral intensity, the characteristic calcite absorption band at 1250–1630 cm^{-1} was utilized as an internal standard for normalization. The results are presented in Figure 6.

 doi:10.20944/preprints202604.1664.v1

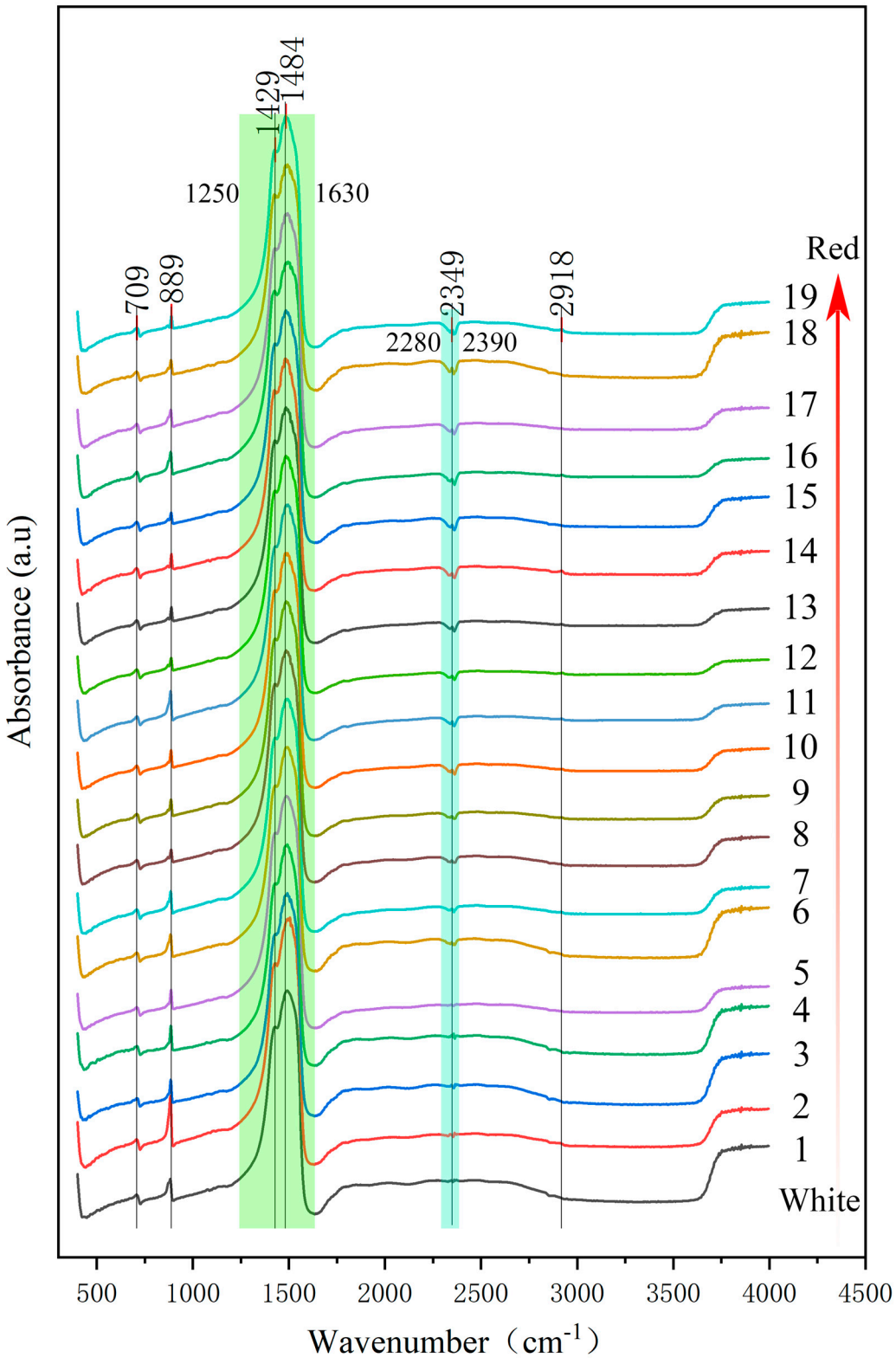

Figure 6. Normalized IR spectra of the precious coral samples (Nos. 1–19).

As shown in Figure 6, the IR spectra of samples No. 1–19 clearly exhibit the characteristic absorptions of both calcite and organic matter. Specifically, the fundamental vibration peaks of calcite are assigned as follows: the peaks at 709 cm^{-1} and 889 cm^{-1} correspond to the in-plane and out-of-plane bending vibrations of (CO_3^{2-}), respectively, while the broad absorption band at 1250–1630 cm^{-1} (the green region) is attributed to the asymmetric stretching vibration of (CO_3^{2-})[5].

 doi:10.20944/preprints202604.1664.v1

In the organic signal region, the characteristic absorption at 2918 cm^{-1} is assigned to the (C–H) stretching vibration. Additionally, a highly anomalous concave structure appears in the 2280–2390 cm^{-1} range (the blue region) of the spectra, within which a signal peak is located at 2349 cm^{-1}.

Additionally, despite careful examination, no signals associated with coloration were identified in the IR reflection spectra.

3.4. Ultraviolet-Visible Spectroscopy

UV-Vis spectroscopy analyzes material composition based on the absorption of ultraviolet and visible light during electronic energy level transitions within molecules or ions. Unlike infrared spectroscopy, which focuses on vibrational energy level transitions, UV-Vis spectroscopy reflects the electronic transition behavior within a substance; thus, the two techniques are highly complementary in molecular characterization. To further elucidate the coloration mechanism of precious coral from the perspective of electronic transitions, UV-Vis spectra of samples No. 1–19 were acquired, and the results are presented in Figure 7.

 doi:10.20944/preprints202604.1664.v1

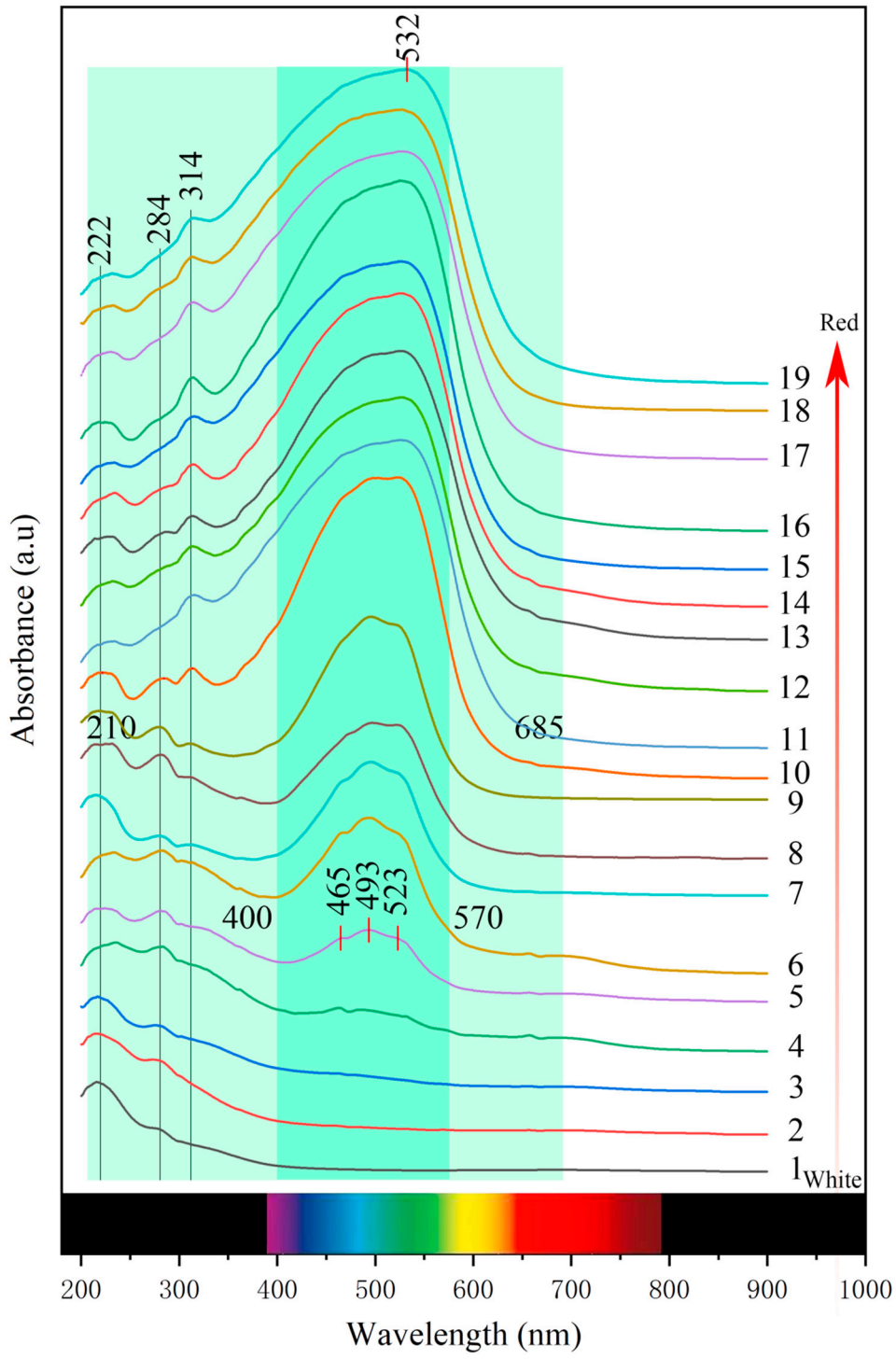

Figure 7. UV-Vis spectra of the precious coral samples (Nos. 1–19).

As shown in Figure 7, the UV-Vis spectra of the precious coral can be divided into two regions: ultraviolet and visible. In the deep ultraviolet region, all 19 samples exhibit a consistent characteristic absorption at 222 nm. In the deep-to-mid ultraviolet range, the light-colored samples (No. 1–12) show a distinct absorption around 284 nm, whereas this signal is not observed in the dark-colored samples (No. 13–19). In fact, the absorption at 284 nm does not actually disappear; rather, it is masked by the intensely broadened absorption band at 532 nm. Because the broad band encompasses the 284 nm region, the latter cannot be effectively resolved in the spectra.

In the mid-to-near ultraviolet range, the absorption band centered at 314 nm exhibits an extremely regular correlation with the color of the samples: this band shows no characteristic

 doi:10.20944/preprints202604.1664.v1

response in the white samples (No. 1–2), appears as a gentle and weak absorption in the light yellow-orange samples (No. 3–6), manifests as a slight protruding absorption in the light red samples (No. 7–10), and significantly intensifies again in the red to dark red samples (No. 10–19). By projecting the integrated intensity of the 314 nm absorption peak against the parameter L*—which serves as an inverse indicator of pigment concentration—to generate Figure 8A, a highly significant negative correlation was found between the two (Spearman's ϱ = -0.900).

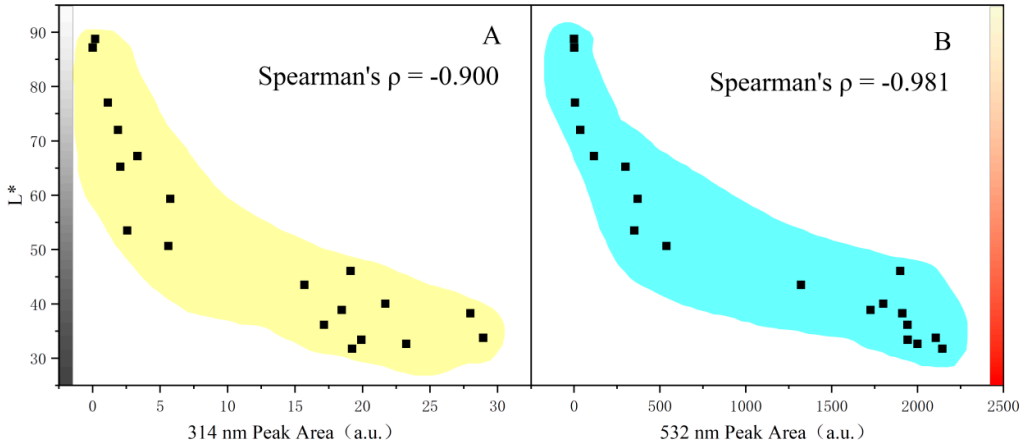

Figure 8. (A) Projection of L* versus the peak intensity at 314 nm; (B) Projection of L* versus the peak intensity at 532 nm. The black-to-white gradient bar on the left indicates the variation in lightness, and the red-to-yellow gradient bar on the right represents the change in sample color.

In the visible light region, as the sample color deepens, a broad absorption band with its maximum at 532 nm appears (the blue region in the figure). Its evolution is highly consistent with the color change: samples No. 1–2 show no characteristic absorption in this range, resulting in total reflection of visible light and appearing white. In samples No. 3–10, the absorption band in the 400–570 nm range emerges and gradually intensifies (the darker blue region) as the color deepens. Within this band, three characteristic absorption peaks can be resolved at 465, 493, and 523 nm, although the maximum absorption point is not yet 532 nm but 493 nm. This spectral region covers the violet, blue, and green light zones; its selective absorption causes the red-orange light to be reflected, which gives the samples their orange-red hue.By the stage of the red to dark red samples (No. 11–19), the absorption band further broadens to the 210–685 nm range, where the three previously distinct peaks overlap and merge, causing the absorption maximum to undergo a redshift to 532 nm. At this point, the visible light outside the red wavelength range is completely absorbed, accompanied by concurrent absorption in the ultraviolet region, and the sample hue shifts entirely from orange-red to red.

By projecting the integrated intensity of the 532 nm absorption band against the parameter L*, which serves as an inverse indicator of pigment concentration, Figure 8B was generated. The two parameters exhibit a highly significant negative correlation (Spearman's ϱ = -0.981).

To illustrate the enhancement and broadening of the 532 nm absorption band alongside the hue variation, the 532 nm band intensity and its long-wavelength absorption edge were plotted against the hue angle (h°) to generate Figure 9.

 doi:10.20944/preprints202604.1664.v1

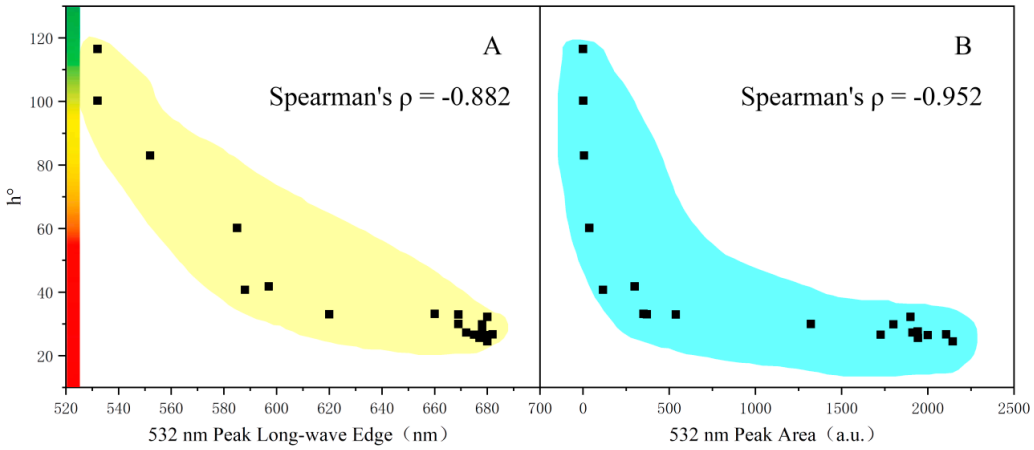

Figure 9. (A) Projection of h° versus the 532 nm peak intensity; (B) Projection of h° versus the long-wavelength edge position of the 532 nm peak.

As shown in Figure 9, the sample hue exhibits a highly significant negative correlation with both the long-wavelength edge position and the peak intensity of the 532 nm absorption band (Spearman's ϱ = -0.882 and -0.952, respectively); that is, the enhancement and broadening of the 532 nm band correspond to a decrease in hue.

3. Discussion

Based on the colors of Samples No. 1 and No. 2, which contain extremely low pigment levels, it can be inferred that in the complete absence of pigment, precious coral would exhibit a white hue with an extremely faint yellowish-green tint (imperceptible to the naked eye). Furthermore, the observation that increasing pigment content decreases the hue value, driving a color transition from orange to red, indicates that the intrinsic color of the pigment in precious coral is red.

In the Raman spectra, Samples 1 and 2 exhibit patterns identical to calcite, while in the FTIR spectra, all samples display calcite signatures. Neither the characteristic peaks of aragonite (around 1085 cm^{-1}) nor the in-plane bending vibration peaks of vaterite (around 745 cm^{-1}) were detected[25]. This cross-validation of Raman and FTIR results further conclusively confirms that the calcareous skeletons of precious corals—regardless of being white or red—are compositionally uniform, consisting exclusively of calcite. This definitively rules out the presence of aragonite or vaterite, delivering a robust refutation of the conventional assertion that "white corals are aragonite, while red corals are calcite."

In the Raman spectra (Figure 4), the visual color demonstrates a synchronous variation with the microscopic signal intensity of polyenes. The integrated intensity of the characteristic peak at 1515 cm^{-1}—representing polyene concentration—shows a highly significant correlation with both the visual color ranking sequence and the lightness value (L*), which represent pigment concentration (Spearman's $|\varrho| > 0.930$). This high degree of statistical consistency explicitly demonstrates that the concentration gradient of polyene substances in precious coral strictly corresponds to its pigment concentration. Consequently, it is conclusively confirmed that this polyene substance acts as the color-inducing pigment of precious coral, thereby substantially bolstering the reliability of previous conclusions[9,12,13].

The color origin of polyene compounds lies in the conjugated system within their molecular backbone, which consists of alternating carbon-carbon single (C-C) and double (C=C) bonds. The π-electron delocalization effect induced by this system significantly reduces the energy gap required for the π-π* transition, causing a shift of the absorbed light wavelength towards longer wavelengths (a bathochromic shift, or red shift)[30]. Once the absorption band enters the visible light region, selective absorption occurs and the complementary color is perceived; the optical mechanism underlying the red coloration of precious coral follows exactly this principle.

 doi:10.20944/preprints202604.1664.v1

In the FTIR spectra (Figure 6), the broad absorption band of calcite in the 1250–1630 cm^{-1} range exhibits splitting, resolving into two distinct peaks at 1429 cm^{-1} and 1484 cm^{-1}, accompanied by a slight splitting phenomenon at the 889 cm^{-1} peak. Fundamentally, this peak splitting reflects lattice distortion, which is hypothesized to arise from the synergistic effects of two mechanisms. First is the ion substitution effect: precious coral belongs to high-Mg calcite, where the incorporation of Mg^{2+} into the lattice by substituting for Ca^{2+} induces local lattice distortion, causing the original vibrational modes to split. Second is biomineralization regulation: the crystallization process of coral calcite is controlled by an organic matrix; the presence and regulatory role of these organics lead to varying degrees of crystal defects or distortions, which subsequently trigger further splitting of the IR absorption peaks.

In Figure 6, a concave feature appears in the 2280–2390 cm^{-1} region (blue area). Natkaniec-Nowak et al. also captured this anomalous spectral band in previous research but did not provide an in-depth analysis[31]. Observing Figure 6 from bottom to top, the depth of this concavity appears to increase with pigment content, superficially suggesting a signal arising from the vibration of a specific functional group within the polyene pigments of the precious coral.

However, subsequent in-depth tracing revealed that this anomalous concavity actually originates from the vibrational absorption interference of CO_2 within the experimental environment (2280–2390 cm^{-1}). The illusion that the concavity "deepens with color intensity" is, in fact, an artifact caused by the testing sequence. Because the samples were analyzed strictly in sequential order from white to red, the CO_2 concentration in the enclosed testing space gradually accumulated due to the operator's respiration as the testing time increased, thereby causing a continuous enhancement of this absorption signal. Therefore, this spectral band has no relevance to the polyene pigments in precious coral and is purely an environmental background interference.

In the UV-Vis spectra (Figure 8), the parameter L*, which inversely represents pigment concentration, shows a highly significant negative correlation with the intensities of the absorption bands at 314 nm and 532 nm (Spearman's $|\varrho| > 0.900$)—equivalently, pigment concentration exhibits a significant positive correlation with the intensities of these two bands. This demonstrates that both absorption bands essentially originate from electronic energy level transitions of the polyene pigments within the precious coral, with the 532 nm band specifically corresponding to the π-π^* electronic transition.

As observed in Figure 9, the intensification and long-wavelength broadening of the 532 nm absorption band are accompanied by a decrease in the hue of the samples. This result reveals the intrinsic mechanism by which the hue of precious coral changes with pigment concentration: as the pigment concentration increases, the 532 nm absorption band undergoes significant enhancement and broadening, which in turn intensifies the absorption in the yellow-orange light region. This intensified absorption reduces the hue value, ultimately driving the color evolution from yellow-orange to red. This spectral pattern explains the phenomenon described earlier (Figure 2B), where the hue decreases as pigment concentration rises.

Concomitant with the enhancement and broadening of the 532 nm absorption band, its absorption maximum undergoes a significant long-wavelength shift (redshifting from 493 nm to 532 nm). Such a peak shift cannot be explained by the concentration change of a single pigment, indicating that there are at least two color-inducing pigments within the precious coral: one with a main absorption peak at 493 nm, and another at 532 nm, whose enrichment dominates the long-wavelength broadening of the absorption band. While further elucidating the intrinsic mechanism of the hue variation in precious coral, this finding also corroborates previous assertions by scholars that the pigments in precious coral are not of a single type [15,18].

In this study, the color, FTIR, Raman, and UV-Vis spectra of precious corals spanning a white-to-red color gradient were systematically collected and analyzed to determine their inorganic composition. The results conclusively demonstrate that polyene pigments act as the color-inducing agents in precious corals and elucidate the intrinsic mechanism driving the hue transition with increasing pigment concentration. Furthermore, corroborative evidence was obtained indicating that

 doi:10.20944/preprints202604.1664.v1

the pigment composition in red corals is not singular. These findings lay a solid foundation for the identification and authentication of precious corals, as well as for further in-depth research into their color genesis.

5. Conclusions

1，The hue of precious coral exhibits a regular shift from orange-red to red as the internal polyene pigment content increases.

2，Cross-validation by Raman spectral characteristic peaks (e.g., 157, 283, 715, 1087, 1441, and 1750 cm^{-1}) and infrared spectral characteristic peaks (e.g., 709, 889, and 1250–1630 cm^{-1}) definitively confirms that the calcareous skeletons of all precious coral samples are composed exclusively of calcite, refuting the conventional assertion that white corals are aragonite while red corals are calcite.

3，The intensity of the characteristic Raman peak at 1515 cm^{-1} for polyene substances exhibits a significant correlation with pigment concentration (as characterized by color and L*; Spearman's $|\varrho| > 0.930$), confirming that this polyene substance is the color-inducing pigment in precious coral. Furthermore, other unassigned signal peaks at 387, 580, 880, 1182, 1395, 1594, and 2986 cm^{-1} also carry structural information about this pigment.

4，In the UV-Vis spectra, both the 314 nm and 532 nm absorption bands originate from electronic transitions within the polyene pigments. Notably, the broad 532 nm absorption band is dominated by π-π* electronic transitions. As the pigment concentration increases, this band exhibits significant broadening and enhancement, accompanied by a synchronous redshift of its absorption maximum. This results in intensified absorption in the yellow-orange light region, elucidating the intrinsic mechanism driving the hue evolution of precious coral from orange to red with increasing pigment concentration. Furthermore, the redshift of the main peak provides additional evidence that the polyene pigments in precious coral are not of a single type.

Author Contributions: Conceptualization, Y.Y., Y.G., Z.H. and J.H.; methodology, Y.Y.; software, Z.H.; validation, Y.Y., Y.G. and J.H.; formal analysis, Y.G.; investigation, Y.Y.; resources, Y.Y.; data curation, Y.Y.; writing—original draft preparation, Y.Y.; writing—review and editing, Y.Y. and J.H; visualization, Y.Y.; supervision, Y.G.; project administration, Y.G.;.All authors have read and agreed to the published version of the manuscript.

Funding: No Funding

Data Availability Statement: We encourage all authors of articles published in MDPI journals to share their research data. In this section, please provide details regarding where data supporting reported results can be found, including links to publicly archived datasets analyzed or generated during the study. Where no new data were created, or where data is unavailable due to privacy or ethical restrictions, a statement is still required. Suggested Data Availability Statements are available in section "MDPI Research Data Policies" at https://www.mdpi.com/ethics.

Acknowledgments: We would like to express our gratitude to the laboratory and all the staff at the School of Gemology, China University of Geosciences (Beijing). We are deeply grateful to Dr. Yuan Ye and Dr. Liu Kang for their invaluable guidance, and to Ruoshui Hu, Pengyu Liu, Ying Yan, and Qing Ai for their assistance.

Conflicts of Interest: The authors declare no conflicts of interest.

Abbreviations

The following abbreviations are used in this manuscript:

MDPI	Multidisciplinary Digital Publishing Institute
DOAJ	Directory of open access journals
TLA	Three letter acronym
LD	Linear dichroism
FTIR	Fourier Transform Infrared Spectroscopy

 doi:10.20944/preprints202604.1664.v1

UV-Vis Ultraviolet-Visible Spectroscopy

References

1. Kennedy, L.; Brigida, C. Italian precious coral. *IMN - Institut des matériaux Jean Rouxel* **2023**, *Vol.59*, 106-107.
2. Borrello, M.A.; Bosch, J.; De Grossi Mazzorin, J.; Estrada Martín, A.; Esteve, X. Les parures néolithiques en corail (Corallium rubrum L.) d'Europe occidentale. *Rivista di scienze preistoriche* **2012**, *Vol.LXII*, 33-66, doi:10.1400/206930.
3. Tsounis, G.; Rossi, S.; Grigg, R.W.; Santangelo, G.; Bramanti, L.; Gili, J.M. The Exploitation and Conservation of Precious Corals. *Departamento de Biología Marina, Institut de Ciències del Mar (CSIC), Passeig Marítim de la Barceloneta, 37-49, Barcelona, 08003, Spain;Institut de CiènciaiTecnologia Ambientals (Universitat Autònoma de* **2010**, *Vol.48*, 161-210, doi:10.1201/ebk1439821169-c3.
4. Ganot Philippe, L.G., Marin Frédéric, Plasseraud Laurent, Allemand Denis, Tambutté Sylvie. An alternative and effective method for extracting skeletal organic matrix adapted to the red coral Corallium rubrum. *Affiliations Unité de Recherche sur la Biologie des Coraux Précieux CSM - CHANEL, Centre Scientifique de Monaco, 8 Quai Antoine 1er, MC 98000, Principality of Monaco, Monaco. Coral Physiology and biochemistry Laboratory, Centre Scientifique* **2022**, *Vol.11*, bio059536, doi:10.1242/bio.059536.
5. Urmos, J.; Sharma, S.K.; Mackenzie, F.T. Characterization of some biogenic carbonates with Raman spectroscopy. *American Mineralogist* **1991**, *Vol.76*, 641-646.
6. Kupka, T.; Buczek, A.; Broda, M.; Szostak, R.; Lin, H.; Fan, L.; Wrzalik, R.; Stobinski, L. Modeling red coral (Corallium rubrum) and African snail (Helixia aspersa) shell pigments: Raman spectroscopy versus DFT studies(Article). *1 Department of Chemistry, University of Opole, 48, Oleska Street, 45-052 Opole, Poland 2 Tatung Technical University, 40, Chungshan North Road, 3rd Section, Taipei 104, Taiwan ROC 3 Institute of Physical Chemistry, Polish* **2016**, *Vol.47*, 908-916, doi:10.1002/jrs.4922.
7. Fox, D.L. Pigmented calcareous skeletons of some corals. *Laboratoire de Spectrochimie Infrarouge et Raman (LP. 2641 CNRS), Université de Lille I, Bâtiment C.5, 59655 Villeneuve d'Ascq Cedex, France (Tel: 20-91-9222)* **1972**, *Vol.43*, 919-927, doi:10.1016/0305-0491(72)90235-0.
8. Cvejic, J.; Tambutté, S.; Lotto, S.; Mikov, M.; Slacanin, I.; Allemand, D. Determination of canthaxanthin in the red coral (Corallium rubrum) from Marseille by HPLC combined with UV and MS detection. *1.Centre Scientifique de Monaco,Monaco,Monaco;2.Aix-Marseille Université, CNRS-UMR 6540 DIMAR, Centre d'Océanologie de Marseille,Marseille,France;3.Institute of Malacology of Tokyo,Nishi-Tokyo City, Tokyo,Japan* **2007**, *Vol.152*, 855-862, doi:10.1007/s00227-007-0738-5.
9. Fritsch, E.; Karampelas, S. Comment on "Determination of carotenoid as the purple pigment in Gorgonia ventalina sclerites using Raman spectroscopy". *1 IMN - Institut des matériaux Jean Rouxel* **2008**, *Vol.71*, 1627, doi:10.1016/j.saa.2008.05.004.
10. Bracco, S.; Fumagalli, P.; Fusi, P.; Santambrogio, C.; Rolandi, V.; Brajkovic, A. Identification of the chromophores in Corallium rubrum gem quality corals by HPLC/UV, ESI-MS and 1H NMR spectroscopy(Article). *Department of Materials Science, University of Milano-Bicocca, Via R. Cozzi 55, Milano, 20125, Italy; Department of Earth and Environmental Sciences, University of Milano-Bicocca, Piazza della Scienza, 1, Milano, 20126, Italy; D* **2016**, *Vol.85*, 83-93, doi:10.2451/2016pm598.
11. Merlin, J.C. Resonance Raman spectroscopy of carotenoids and carotenoid-containing systems. *Pure and Applied Chemistry* **1985**, *Vol.57*, 785-792, doi:10.1351/pac198557050785.
12. Merlin, J.C.; Delé-Dubois, M.L. Resonance Raman characterization of polyacetylenic pigments in the calcareous skeleton. *Laboratoire de Spectrochimie Infrarouge et Raman (LP. 2641 CNRS), Université de Lille I, Bâtiment C.5, 59655 Villeneuve d'Ascq Cedex, France (Tel: 20-91-9222)* **1986**, *Vol.84*, 97-103, doi:10.1016/0305-0491(86)90277-4.
13. Smith, C.P.; McClure, S.F.; Eaton-Magana, S.; Kondo, D.M. PINK-TO-RED CORAL: A GUIDE TO DETERMINING ORIGIN OF COLOR. *American Gemological Laboratories (AGL), New York City;GIA Laboratory in Carlsbad;GIA Laboratory, New York;GIA Laboratory, New York* **2007**, *Vol.43*, 4-15, doi:10.5741/gems.43.1.4.

 doi:10.20944/preprints202604.1664.v1

14. Metiyier, B.; Karampelas, S.; Rondeau, B.; Andouche, A.; Fritsch, E. Identification of the Endangered Pink-to-Red Stylaster Corals by Raman Spectroscopy. *IMN - Institut des matériaux Jean Rouxel* **2009**, *Vol.45*, 48-52, doi:10.5741/gems.45.1.48.
15. Yang, Y.; Guo, Y.; Zhang, Y.; Zou, Y.; Wei, J.; Liang, L. Contribution of coral composition to color red in the uniform color space CIE 1976L*a*b. *China Univ Geosci, Sch Gemmol, Beijing 100083, Peoples R China.;Dehong Teachers Coll, Dept Sci & Technol, Mangshi 678400, Peoples R China.;Shanghai Normal Univ, Sch Foreign Language, Shanghai 200234, Peoples R China.;Chi* **2019**, *Vol.168*, 384-393, doi:10.5004/dwt.2019.24212.
16. Bergamonti, L.; Bersani, D.; Mantovan, S.; Lottici, P.P. Micro-Raman investigation of pigments and carbonate phases in corals and molluscan shells. *;[1] Univ Parma, Dept Chem, I-43124 Parma, Italy [2] Univ Parma, Phys & Earth Sci Dept, I-43124 Parma, Italy* **2013**, *Vol.25*, 845-853, doi:10.1127/0935-1221/2013/0025-2318.
17. Brambilla, L.; Tommasini, M.; Zerbi, G.; Stradi, R. Raman spectroscopy of polyconjugated molecules with electronic and mechanical confinement: The spectrum of Corallium rubrum(Article). *1 Department of Chemistry, University of Opole, 48, Oleska Street, 45-052 Opole, Poland 2 Tatung Technical University, 40, Chungshan North Road, 3rd Section, Taipei 104, Taiwan ROC 3 Institute of Physical Chemistry, Polish* **2012**, *Vol.43*, 1449-1458, doi:10.1002/jrs.4057.
18. Kupka, T.; Lin, H.; Stobinski, L.; Chen, C.; Liou, W.; Wrzalik, R.; Flisak, Z. Experimental and theoretical studies on corals. I. Toward understanding the origin of color in precious red corals from Raman and IR spectroscopies and DFT calculations. *1 Department of Chemistry, University of Opole, 48, Oleska Street, 45-052 Opole, Poland 2 Tatung Technical University, 40, Chungshan North Road, 3rd Section, Taipei 104, Taiwan ROC 3 Institute of Physical Chemistry, Polish* **2010**, *Vol.41*, 651-658, doi:10.1002/jrs.2502.
19. Ishikawa, M.; Kagi, H.; Sasaki, T.; Endo, K. Chemical basis of molluscan shell colors revealed with in situ micro-Raman spectroscopy. *1 Department of Chemistry, University of Opole, 48, Oleska Street, 45-052 Opole, Poland 2 Tatung Technical University, 40, Chungshan North Road, 3rd Section, Taipei 104, Taiwan ROC 3 Institute of Physical Chemistry, Polish* **2019**, *Vol.50*, 1700-1711, doi:10.1002/jrs.5708.
20. Fernández-Manteca, M.G.; García García, B.; Gómez-Galdós, C.; Mirapeix, J.; Arniz-Mateos, R.; García-Escárzaga, A.; Gutiérrez-Zugasti, I.; Algorri, J.F.; López-Higuera, J.M.; Ocampo-Sosa, A.A.; et al. Structural Pattern Analysis in Patella vulgata Shells Using Raman Imaging. *Photonics Engineering Group, Universidad de Cantabria, Santander, 39005, Spain;Instituto de Investigación Sanitaria Valdecilla (IDIVAL), Santander, 39011, Spain;CIBER de Bioingeniería, Biomateriales y Nanomedicina (CIBER-B* **2025**, *Vol.15*, 5180, doi:10.3390/app15095180.
21. Oikawa, K.; Takayanagi, H.; Fujioka, H.; Takizawa, M.; Arakane, M.; Kouketsu, Y.; Charoentitirat, T.; Hara, H.; Yamamoto, K.; Abe, O.; et al. New screening method for well-preserved brachiopod shells and shell portions for paleoenvironmental analysis: Raman spectroscopy. *Department of Earth Science, Graduate School of Science, Tohoku University, Sendai, 980-8578, Japan;Advanced Institute for Marine Ecosystem Change (WPI-AIMEC), Tohoku University, Sendai, 980-8578, Japan;Department* **2026**, *Vol.13*, doi:10.1186/s40645-026-00811-0.
22. Fang, S.; Yan, X.; Kong, Y.; Zheng, T.; Zhu, P.; Sun, Q.; Zhou, Y.; Yan, J. Dynamic UV-Vis Diffuse Reflection and Raman Spectral Characteristics of Seawater-Cultured Golden Pearls. *Zhejiang Fangyuan Test Group Co., Ltd., Hangzhou 310013, Zhejiang, China College of Materials Science and Engineering, Zhejiang University of Technology, Hangzhou 310014, Zhejiang, China College of Information and Electr* **2022**, *Vol.59*, 1930004, doi:10.3788/lop202259.1930004.
23. Gao, J.; Zhang, J.; Wu, W.; Yen, C.K.; Su, W. Polarized Raman spectroscopy reveals unaligned orientation in pearls. *1 Department of Chemistry, University of Opole, 48, Oleska Street, 45-052 Opole, Poland 2 Tatung Technical University, 40, Chungshan North Road, 3rd Section, Taipei 104, Taiwan ROC 3 Institute of Physical Chemistry, Polish* **2023**, *Vol.54*, 371-378, doi:10.1002/jrs.6492.
24. Nozomu IWASAKI, H.H., Atsushi SUZUKI, Taro MORIWAKI, Yuka IKEMOTO. Structural Analysis of Precious Coral Carbonate Layers Using Synchrotron Radiation-infrared Rays. *Rissho University, Kumagaya-shi, Saitama 360-0194, 1700, Magechi, Japan;Institute of Science and Engineering, Kanazawa University, Kakuma, Kanazawa-shi, Ishikawa 920-1192, Japan;Institute of Geology and Geoinformation, National Institute* **2014**, *Vol.63*, 593-602, doi:10.2116/bunsekikagaku.63.593.

 doi:10.20944/preprints202604.1664.v1

25. Vongsavat, V.; Winotai, P.; Meejoo, S. Phase transitions of natural corals monitored by ESR spectroscopy. *Department of Chemistry, Faculty of Science, Mahidol University, Rama VI Road, Rajathevi, Bangkok 10400, Thailand* **2006**, *Vol.243*, 167-173, doi:10.1016/j.nimb.2005.07.197.
26. Ghasemi, J.B.; Khani, S.; Piravi-Vanak, Z. Development of a Computer Vision System for the Classification of Olive Oil Samples with Different Harvesting Years and Estimation of Chlorophyll and Carotenoid Contents: A Comparison of the Proposed Method's Efficiency with Uv-Vis Spectroscopy. *Department of Chemistry, Faculty of Science, University of Tehran, Iran;Food Technology and Agricultural Products Research Center, Standard Research Institute (SRI), Karaj, Iran* **2023**, doi:10.2139/ssrn.4604781.
27. Mahy, M.; Eycken, L.V.; Oosterlinck, A. Evaluation of Uniform Color Spaces Developed after the Adoption of CIELAB and CIELUV. *Seongkwan Hong (Department of Architectural Engineering, Sejong University) ; Intae Kim (Department of Architectural Engineering, Sejong University) ; Hyunsun Kim (Department of Architectural Engineering, Sejong Universit* **1994**, *Vol.19*, 105-121, doi:10.1111/j.1520-6378.1994.tb00070.x.
28. Colorimetry - Part 4: CIE 1976 L*a*b* colour space (ISO/CIE 11664-4:2019). 17.
29. Floquet, N.; Vielzeuf, D.; Ferry, D.; Ricolleau, A.; Heresanu, V.; Perrin, J.; Laporte, D.; Fitch, A. Thermally Induced Modifications and Phase Transformations of Red Coral Mg-Calcite Skeletons from Infrared Spectroscopy and High Resolution Synchrotron Powder Diffraction Analyses. *CINaM UMR7325, Aix-Marseille Université, CNRS, Campus de Luminy, Case 913, 13288 Marseille, France;Laboratoire Magmas et Volcans, Université Blaise Pascal-CNRS-IRD, OPGC, 5 rue Kessler, 63038 Clermont Ferrand, France;European Syn* **2015**, *Vol.15*, 3690-3706, doi:10.1021/acs.cgd.5b00291.
30. G., B. Structure and properties of carotenoids in relation to function. *Department of Biochemistry, University of Liverpool, Liverpool, United Kingdom Department of Biochemistry, University of Liverpool, P.O. Box 117, Liverpool L69 3BX, United Kingdom* **1995**, *Vol.9*, 1551-1558, doi:10.1096/fasebj.9.15.8529834.
31. Natkeniec-Nowak, L.; Dumanska-Slowik, M.; Fijal, J.; Krawczyk, A. Application of mineralogical methods to the investigation of some gem-quality corals. *Aix Marseille Université, CNRS, Centre Interdisciplinaire de NanoScience de Marseille, UMR 7325, 13288 Marseille, France CNRS-Sorbonne Université, Laboratoire d'Ecogéochimie des Environnements Benthiques, LECOB,* **2010**, *Vol.31*, 226-234, doi:10.15506/jog.2009.31.5.226.